

Dynamic analysis of chaotic maps as complex networks in the digital domain

Chengqing Li, *Senior Member, IEEE*, Bingbing Feng, Shujun Li, *Senior Member, IEEE*, Juergen Kurths, Guanrong Chen, *Fellow, IEEE*

Abstract—Chaotic dynamics is widely used to design random number generators. This paper aims to study the dynamics of chaotic maps in a digital finite-precision domain. Differing from the traditional approaches treating a digital chaotic map as a black box with different explanations according to the test results of the output, the dynamical properties of such chaotic maps are explored in an fixed-point arithmetic domain, using the Logistic map and the Tent map as representative examples, from a new perspective with a corresponding state-mapping network (SMN). In SMN, every possible value is considered as a node and the mapping relationship between any pair of nodes works just like a directed edge. The scale-free properties of SMN are proved. The analytic results can be further extended to the scenario of floating-point arithmetic and for other chaotic maps. Understanding the network structure of SMN of a chaotic map in the digital computers can facilitate counteracting the undesirable dynamics degenerations of digital chaotic maps in finite-precision domains, helping also classify and improve the randomness of pseudo-random number sequences generated by iterating chaotic maps.

Index Terms—Chaotic map, complex network, dynamics degradation, floating-point arithmetic, pseudorandom number generator, PRNS, randomness.

I. INTRODUCTION

DYNAMICS of chaos in the infinite-precision domain is a fundamental topic in the fields of mathematical chaos theory and nonlinear sciences. Yet, the implementation of a chaotic system in a digital device is always an inevitable problem withholding its real applications [1], [2]. Under the joint influence of round-off error and truncation error (algorithmic error) in the finite-precision domain (or a finite-state machine), a resultant digital orbit is off-tracked from the theoretical one [3], [4]. Based on the well-known *shadowing lemma*, many believed that any pseudo-random number sequence generated by iterating a chaotic map retains the complex dynamics of

the original chaotic map to a high extent [5]. However, it was found that the dynamics of a digital chaotic map are definitely degraded to some degree [6]. In 1988, Yorke *et al.* investigated the period distribution of an orbit of the Ikeda map, starting from a specific initial point under various round-off precisions and found that the expected number of periodic orbits is scaled to the precision [7]. In [8], a set of objective metrics were proposed to measure the degree of dynamics degradation of piecewise-linear chaotic maps. In 1991, Chua [9] suggested that a real digital filter can exhibit near-chaotic behaviors if its wordlength is sufficiently large (*e.g.*, larger than 16 bits). In [10], Kocarev defined *digital chaos* via convergence of its maximum Lyapunov exponent to a positive number when the size of the discrete space tends to infinity.

In retrospect, the seemingly complex dynamics of chaos has been very appealing for random number generation [11]–[13] and random permutation [14]. In fact, in 1947, von Neumann already suggested using the Logistic map as a pseudo-random number generator (PRNG) [15]. Since then, a large number of PRNG have been proposed based on various chaotic maps and their variants, *e.g.*, the Logistic map [5], [13], [16]–[18], the Tent map [12], [14], [19], the Sawtooth map [20], the Rényi chaotic map [21], and the Cat map [22]. In addition, chaos theory was widely used to design hash functions and encryption schemes. However, as reviewed in [23], any dynamics degradation of digital chaos may facilitate thwarting security of the supported schemes.

Due to the “pigeonhole principle” and a limited possible number of a digital state, the orbit generated by iterating a chaotic map from any initial state in the digital domain will definitely enter a periodic loop after a transient process, referring to the general *cycle detection* problem about periodic functions, as discussed in [24], [25]. The existence of a network relationship among all possible states of a given chaotic map in the digital domain was often ignored [26], instead with focus on statistics along the orbit (path) on the network. When the orbits of the Logistic map are computed in 64-bit floating-point precision, by statistical analysis it was shown how the errors change with respect to the control parameters [3]. In [22], [27], period distribution of the generalized discrete Arnold cat map was precisely derived. Furthermore, the maximum period of the sequences generated by iterating the Logistic map over the field \mathbb{Z}_3^n was derived in [28]. In [29], the influences of different rounding methods on the transient lengths and cycle lengths were analyzed

This work was supported by DAAD/K.C.Wong Fellowship (no. 91664078), the National Natural Science Foundation of China (no. 61532020, 61772447), Royal Society, UK under the Grant Ref. 1E111186, and the Hong Kong Research Grants Council under the GRF Grant CityU 11234916.

C. Li is with School of Computer Science and Electronic Engineering, Hunan University, Changsha 410082, Hunan, China (DrChengqingLi@gmail.com).

B. Feng is with College of Information Engineering, Xiangtan University, Xiangtan 411105, Hunan, China.

S. Li is with Department of Computing, University of Surrey, Guildford, Surrey, GU2 7XH, UK.

J. Kurths is with Potsdam Institute for Climate Impact Research, D-14415 Potsdam, Germany.

G. Chen is with Department of Electronic Engineering, City University of Hong Kong, Hong Kong SAR, China.

experimentally. The influences caused by control parameters were further analyzed in [30]. In [6], the periods and cycles of the Logistic map are exhaustively calculated in 32-bit floating point precision using high-throughput computing.

Recently, complex networks as an emerging standalone research field has been able to provide useful tools for studying the dynamics of chaotic times series, starting from the pioneering work [31]. Some earlier works on the dynamics of digital chaos via studying the state-mapping network (or state transition diagram and functional graph), composing of relationships between every pair of states, fall into the scope of complex networks. In 1986, Binder [32] drew the state network of the Logistic map in the 5-bit fixed-point arithmetic domain and reported that the counterparts of some metrics for measuring dynamics in continuous chaos, such as Lyapunov exponent and entropy, work just as well. In [33], he further experimentally studied how the number of limit cycles and the size of the longest cycle change with the fixed-point precision. Later, an analytical framework was proposed for recurrence network analysis of chaotic time series [34], [35]. In [36], the dynamics of time series generated by cellular automata was classified by two parameters of an associate network. In [37], an orbit of a state-mapping network (SMN) was transformed into a network via horizontal visibility. It was found that the network entropy can mimic the Lyapunov exponent of the original map in a subtle level. In [38]–[41], a mapping network among sub-intervals was established to explore the coherence between network parameters and some well-recognized metrics characterizing chaotic dynamics. In [42], the relative frequency of different 4-node subgraphs (motifs) of SMN of some conventional chaotic maps and flows was used to discriminate the underlying chaotic systems.

To counteract dynamics degradation, many methods have been proposed, including adopting higher precision [9], perturbing chaotic states [16]–[18], [43], perturbing control parameters [44], and cascading two or more chaotic maps [45], switching multiple chaotic maps [46], [47], and feedback control [13], [48]. Most of these works claimed that the improved discrete chaotic maps can work as good alternatives of the classic PRNG, by showing that their results pass typical randomness test suites. Nevertheless, there is still a need of a simple universal tool to compare the randomness performances of the chaotic-map-based PRNG.

It has been observed that, in the field of nonlinear sciences, many did not care about how their computers perform floating-point arithmetic domain, but implemented a chaotic system in the computer just like a black box. Thus, the real structure of the chaotic map implemented in the computer remains mysterious, in which some important details occurring with a very low probability were omitted by a limited number of random experiments. To improve such a situation, this paper studies the properties of SMN generated by iterating a chaotic map in the digital domain: every representable value in the definition domain of the chaotic map is considered as a node, while a directed edge between a pair of nodes is built if and only if the former node is mapped to the latter one by the chaotic map. Using the Logistic map and the Tent map as illustrative examples, the dynamical properties of chaotic

maps in the fixed-point arithmetic domain are disclosed by studying their corresponding SMN. The scale-free properties of SMN are mathematically proved. The relationship between SMN obtained in a floating-point arithmetic domain and that in a fixed-point arithmetic domain is revealed. Finally, it will be shown that SMN can work as fingerprints of chaos-based PRNG to coarsely evaluate their randomness.

The remainder of the paper is organized as follows. Section II performs network analysis of the SMN of the Logistic map and the Tent map in the fixed-point arithmetic domain. Section III presents an analysis of the SMN of the two maps in the floating-point arithmetic domain. An application of SMN to the evaluation of PRNG is discussed in Sec. IV. The last section concludes the investigation.

II. STATE-MAPPING NETWORK OF DIGITAL CHAOTIC MAPS IN THE FIXED-POINT ARITHMETIC DOMAIN

A. Basic properties of chaotic maps implemented in fixed-point arithmetic precision

Given a map $f: [0, 1] \rightarrow [0, 1]$ and a computing domain of fixed-point arithmetic precision n , with a specified quantization scheme, the associate *state-mapping network* F_n can be built in the following way: the 2^n possible states are viewed as 2^n nodes; every pair of nodes with labels i and j is linked with a directed edge if $f(i/2^n) = j/2^n$. Let $f_n(i)$ denote the original value corresponding to the node with label i in F_n before the final quantization step, namely,

$$F_n(i) = \text{R}(f_n(i) \cdot 2^n),$$

where $\text{R}(\cdot)$ is an integer quantization function, *e.g.* floor, ceil, and round (here and throughout, only round quantization is considered.).

Then, the following three properties on the relationship between F_n and F_{n+1} can be easily verified.

Property 1. *The node with the label $(2i)$ in F_{n+1} and that with the label i in F_n satisfy*

$$F_{n+1}(2i) - 2F_n(i) = \begin{cases} 1 & \text{if } r_n \in [0.25, 0.5); \\ -1 & \text{if } r_n \in [0.5, 0.75); \\ 0 & \text{otherwise,} \end{cases} \quad (1)$$

where

$$r_n = \text{frac}(f_n(i) \cdot 2^n),$$

$\text{frac}(x) = x - \lfloor x \rfloor$, $i \in \{0, \dots, 2^n\}$, and $\lfloor x \rfloor$ returns the largest integer less than or equal to x .

Proof. Since $F_{n+1}(2i) = \text{R}(2 \cdot f_{n+1}(2i) \cdot 2^n)$ and

$$f_{n+1}(2i) \equiv f_n(i),$$

the proof of this property is straightforward using

$$\text{R}(2x) = 2 \cdot \text{R}(x) + \begin{cases} 0 & \text{if } 0 \leq \text{frac}(x) < 0.25; \\ 1 & \text{if } 0.25 \leq \text{frac}(x) < 0.5; \\ -1 & \text{if } 0.5 \leq \text{frac}(x) < 0.75; \\ 0 & \text{if } 0.75 \leq \text{frac}(x) \leq 1. \end{cases}$$

□

Property 2. *The node with the label $(2i + 1)$ in F_{n+1} and that with the label i in F_n satisfy*

$$\begin{aligned} & |F_{n+1}(2i + 1) - 2 \cdot F_n(i)| \\ & \leq |\mathbf{R}((f_{n+1}(2i + 1) - f_{n+1}(2i)) \cdot 2^{n+1})| \\ & \quad + \begin{cases} 2 & \text{if } r_n \in [0.25, 0.75]; \\ 1 & \text{otherwise,} \end{cases} \end{aligned} \quad (2)$$

and $i \in \{0, \dots, 2^n - 1\}$.

Proof. According to the triangular inequality, one has

$$\begin{aligned} & |F_{n+1}(2i + 1) - 2 \cdot F_n(i)| \leq \\ & |F_{n+1}(2i + 1) - F_{n+1}(2i)| + |F_{n+1}(2i) - 2 \cdot F_n(i)|. \end{aligned} \quad (3)$$

Utilizing the property of the integer quantization function

$$|\mathbf{R}(x) - \mathbf{R}(y)| \leq |\mathbf{R}(x - y)| + 1, \quad (4)$$

one obtains

$$\begin{aligned} & |F_{n+1}(2i + 1) - F_{n+1}(2i)| \\ & = |\mathbf{R}(f_{n+1}(2i + 1) \cdot 2^{n+1}) - \mathbf{R}(f_{n+1}(2i) \cdot 2^{n+1})| \\ & \leq |\mathbf{R}(f_{n+1}(2i + 1) \cdot 2^{n+1} - f_{n+1}(2i) \cdot 2^{n+1})| + 1 \end{aligned} \quad (5)$$

Incorporating the above inequality and Eq. (1) into inequality (3), the property is proved. \square

Property 3. *The node with the label $(2i - 1)$ in F_{n+1} and that with the label i in F_n satisfy*

$$\begin{aligned} & |F_{n+1}(2i - 1) - 2 \cdot F_n(i)| \\ & \leq |\mathbf{R}((f_{n+1}(2i - 1) - f_{n+1}(2i)) \cdot 2^{n+1})| \\ & \quad + \begin{cases} 2 & \text{if } r_n \in [0.25, 0.75]; \\ 1 & \text{otherwise,} \end{cases} \end{aligned} \quad (6)$$

and $i \in \{1, \dots, 2^n\}$.

Proof. As the proof is very similar to that of Property 2, it is omitted. \square

B. SMN of the digital Logistic map

In the digital domain with fixed-point precision n , the Logistic map

$$f(x) = \mu \cdot x \cdot (1 - x) \quad (7)$$

becomes

$$f_n(i) = (N_\mu / 2^{n_\mu}) \cdot (i / 2^n) \cdot (1 - i / 2^n), \quad (8)$$

where N_μ is an odd integer in $\{0, \dots, 2^{n_\mu+2}\}$, $\mu = N_\mu / 2^{n_\mu}$, and $n_\mu \leq n$. To facilitate the following discussion, we draw the SMN of the Logistic map, F_n^* , with a fixed control parameter in the three arithmetic domains shown in Fig. 1a), b), and c), respectively.

By observing Fig. 1, the following basic characteristics of SMN of the digital map can be noticed:

- The whole SMN is composed of a small number of *weakly connected components*, which are maximal subgraphs of a directed graph satisfying that, for every pair of nodes u, v in any subgraph, there is an undirected path from u to v and a directed path from v to u .

- Each weakly connected component has one and only one self-loop (an edge connecting a node to itself) or cycle (a sequence of nodes starting and ending at the same node such that, for every two consecutive nodes in the cycle, there exists an edge directed from the former node to the later one.)
- Any node is linked to the cycle of the associated weakly connected component via a *transient* process.

From Fig. 1a), b), c), one can further observe a special property of SMN of the Logistic map: one weakly connected component dominates the whole SMN and there is a clear decreasing order among all the weakly connected components [49]. More precisely, the size of the component accounts for more than half of the size of the whole network.

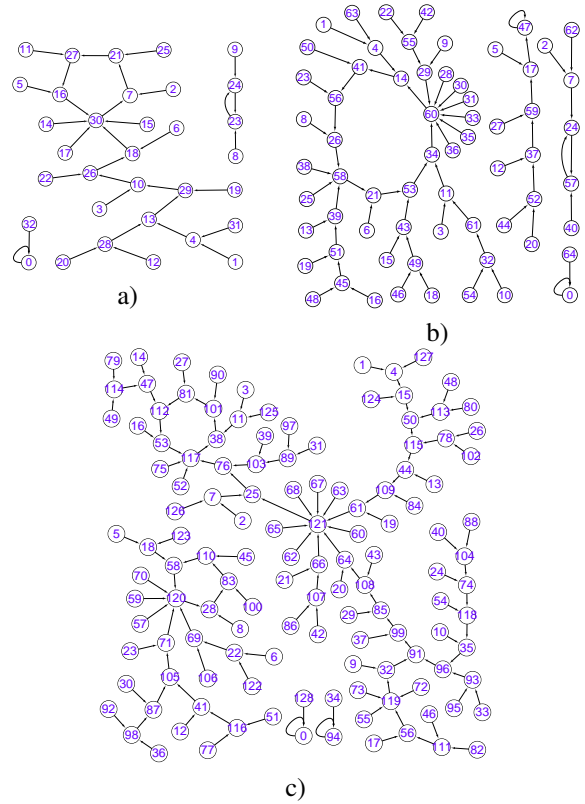


Fig. 1. The SMN of the Logistic map with $\mu = 121/2^5$: a) 5-bit precision; b) 6-bit precision; c) 7-bit precision.

Corollary 1. *The nodes of odd label numbers in the state network of F_{n+1}^* and that in the state network of F_n^* satisfy*

$$|F_{n+1}^*(2i + 1) - 2 \cdot F_n^*(i)| \leq \begin{cases} 6 & \text{if } r_n \in [0.25, 0.75]; \\ 5 & \text{otherwise,} \end{cases}$$

where $i \in \{0, \dots, 2^n - 1\}$, and $n \geq 3$.

Proof. By putting Eq. (8) into inequality (2), one gets

$$\begin{aligned} & |F_{n+1}^*(2i + 1) - 2 \cdot F_n^*(i)| \\ & \leq |\mathbf{R}((N_\mu / 2^{n_\mu+2}) \cdot (4 - (1 + 4i) / 2^{n-1}))| + \\ & \quad \begin{cases} 2 & \text{if } r_n \in [0.25, 0.75]; \\ 1 & \text{otherwise,} \end{cases} \end{aligned}$$

based on Property 2.

As $(N_\mu/2^{n_\mu+2}) \in [0, 1]$, one furthermore has

$$\begin{aligned} & |F_{n+1}^*(2i+1) - 2 \cdot F_n^*(i)| \\ & \leq \left| \mathbb{R} \left(4 - (1 + 4i)/2^{n-1} \right) \right| + \\ & \quad \begin{cases} 2 & \text{if } r_n \in [0.25, 0.75]; \\ 1 & \text{otherwise,} \end{cases} \\ & \leq \begin{cases} 6 & \text{if } r_n \in [0.25, 0.75]; \\ 5 & \text{otherwise.} \end{cases} \end{aligned}$$

□

Property 4. SMN $F_{n_\mu}^*$ has dominating influence on F_n^* .

Proof. From Property 1 and Corollary 1, it is clear that F_n^* can be considered as the result obtained by incrementally expanding F_j^* within a fixed small scope from $j = n_\mu$ to n . Furthermore, the error in each expansion step falls into a small scope. So, the initial structure of $F_{n_\mu}^*$ has a critical influence on F_n^* . □

From the proof of Corollary 1, one can see that the upper bound of $|F_{n+1}^*(2i+1) - 2 \cdot F_n^*(i)|$ depends on the value of i and N_μ . Figure 2a) depicts the values of $|F_{n+1}^*(2i+1) - 2 \cdot F_n^*(i)|$ and $F_{n+1}^*(2i) - 2F_n^*(i)$ for every node shown in Fig. 1a). The corresponding data for the nodes shown in Fig. 1b) are plotted in Fig. 2b), to further demonstrate the differences between F_n^* and F_{n+1}^* .

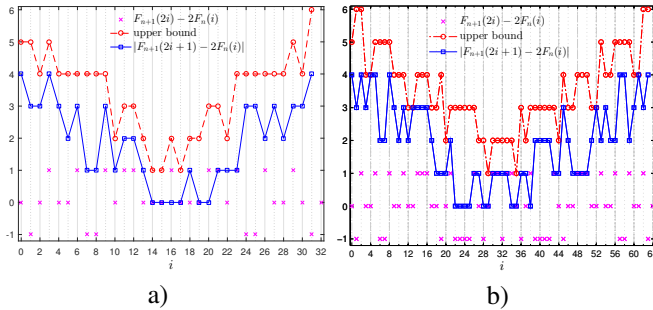


Fig. 2. Distribution of the difference between F_n^* and F_{n+1}^* : a) $n = 5$; b) $n = 6$.

Theorem 1. The cumulative in-degree distribution of the SMN F_n^* satisfies

$$P(k) = \left(\frac{2}{\mu k} - \frac{k}{2^{n+1}} \right)^2.$$

Proof. In a computing domain of fixed-point arithmetic precision n with a specified quantization scheme, the definition domain and value domain of any 1-D map are both divided into intervals of fixed length $\Delta = 1/2^n$.

As demonstrated by Fig. 3, for the interval to which $y_0 = f(x_0)$ belongs, the number of intervals owning pre-image of y_0 in the neighborhood of x_0 is

$$c = \left\lceil \frac{|x - f^{-1}(f(x) - \Delta)|}{\Delta} \right\rceil,$$

□

where $\lceil x \rceil$ gives the smallest integral value not less than the argument. Since the Logistic map (7) has a symmetric property, namely,

$$f(x) = f(1-x), \quad (9)$$

the in-degree of the node corresponding to $y = f(x)$ is double of that in the left half part of the definition domain.

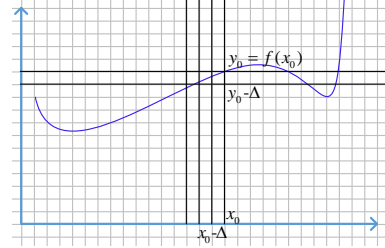


Fig. 3. Demonstration of counting the number of preimages of a map in the digital domain.

In the interval $[0, 1/2]$, the inverse function of map (7) is

$$f^{-1}(y) = (1 - \sqrt{1 - 4y/\mu})/2.$$

Furthermore, $f'(x) = \mu \cdot (1 - 2x) > 0$ for $x \in [0, 1/2)$, and $f(x)$ monotonously increases with respect to x . So, one has the in-degree of the node to which y belongs, as

$$\begin{aligned} k &= 2 \cdot \left\lceil \frac{f^{-1}(y) - f^{-1}(y - 1/2^n)}{2^{-n}} \right\rceil \\ &= 2 \cdot \left\lceil \frac{\sqrt{1 - 4(y - 1/2^n)/\mu} - \sqrt{1 - 4y/\mu}}{2^{1-n}} \right\rceil. \end{aligned}$$

From this equation, one gets

$$y = \frac{\mu}{4} - \frac{1}{\mu \cdot (k + \epsilon)^2} - \frac{\mu \cdot (k + \epsilon)^2}{2^{2n+4}} + 2^{-n-1}, \quad (10)$$

where ϵ is the change caused by the quantization function, and $0 \leq \epsilon < 0.5$. As the relative influence of ϵ is very small, such similar cases are neglected in the following discussion.

As $f''(x) \equiv -2\mu$ for $x \in [0, 1/2]$ and the in-degree corresponding to y monotonously decreases as it increases from zero to the maximum value $f(1/2) = \mu/4$, the rank of the state y is

$$r = \left\lceil \frac{\mu/4 - y}{1/2^n} \right\rceil,$$

and the number of nodes

$$N = \left\lceil \frac{\mu/4}{1/2^n} \right\rceil.$$

According to the definition of the cumulative in-degree distribution, one has

$$P(k) = 1 - \frac{4y}{\mu}.$$

Incorporating Eq. (10) into the above equation, one obtains

$$P(k) = \left(\frac{2}{\mu k} - \frac{k}{2^{n+1}} \right)^2.$$

□

Obviously, $P(k)$ monotonously increases with respect to n . So, by increasing the value of n , the cumulative in-degree distribution of SMN for the Logistic map tends to its limit: $\lim_{n \rightarrow \infty} P(k) = \frac{4}{\mu^2 k^2}$. To verify this, we draw the cumulative in-degree distributions of SMN $F_5^* \sim F_{20}^*$ as in Fig. 4, where N is fixed to be 2^{20} , to clearly demonstrate the evolution of the distributions. The corresponding in-degree distributions are shown in Fig. 5, which agree with Corollary 2.

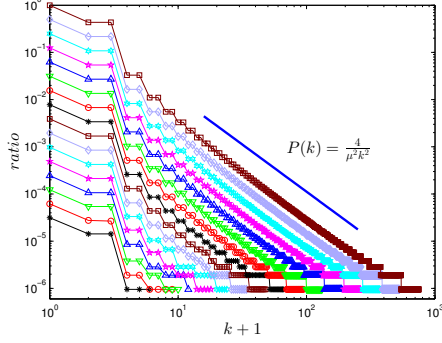


Fig. 4. Cumulative in-degree distributions of SMN $F_5^* \sim F_{20}^*$, where $\mu = \frac{121}{2^5}$.

Corollary 2. *The in-degree distribution of the SMN F_n^* satisfies*

$$p(k) \doteq \frac{16(k+1)}{\mu^2 k^2 (k+2)^2}.$$

Proof. Due to the symmetry property of the Logistic map, the in-degree of its SMN is always even except the one corresponding to the critical point $f(1/2)$.

According to the definition of the cumulative in-degree distribution, the in-degree distribution $p(k)$ can be calculated as

$$p(k) = P(k) - P(k+2).$$

So, one has

$$\begin{aligned} p(k) &= \left(\frac{2}{\mu k} - \frac{k}{2^{n+1}} \right)^2 - \left(\frac{2}{\mu(k+2)} - \frac{k+2}{2^{n+1}} \right)^2 \\ &= (k+1) \left(\frac{16}{\mu^2 k^2 (k+2)^2} - \frac{1}{2^{2n}} \right). \end{aligned}$$

Obviously, $p(k)$ monotonously tends to its limit value: $\lim_{n \rightarrow \infty} p(k) = \frac{16(k+1)}{\mu^2 k^2 (k+2)^2}$ as n increases. \square

C. SMN of the digital Tent map

In the same digital domain discussed in the last subsection, the Tent map $f(x) = \mu \cdot (1 - 2|x - 1/2|)$ becomes

$$f_n(i) = ((N_\mu / 2^{n\mu}) \cdot (1 - 2|(i/2^n) - 1/2|)). \quad (11)$$

To facilitate the following discussion, we draw the SMN of the Tent map, F_n^* , with $\mu = 31/2^5$ in the domains of fixed-point 5-bit and 6-bit, respectively, in Fig. 6a) and b).

Corollary 3. *The nodes of the odd label numbers in the state network of F_{n+1}^* and that in the state network of F_n^* satisfy*

$$|F_{n+1}^*(2i+1) - 2 \cdot F_n^*(i)| \leq \begin{cases} 4 & \text{if } r_n \in [0.25, 0.75); \\ 3 & \text{otherwise,} \end{cases}$$

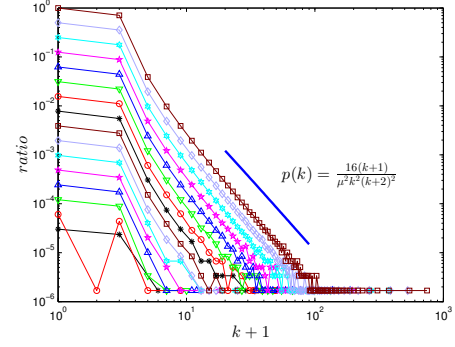


Fig. 5. In-degree distributions of SMN $F_5^* \sim F_{20}^*$, where $\mu = \frac{121}{2^5}$

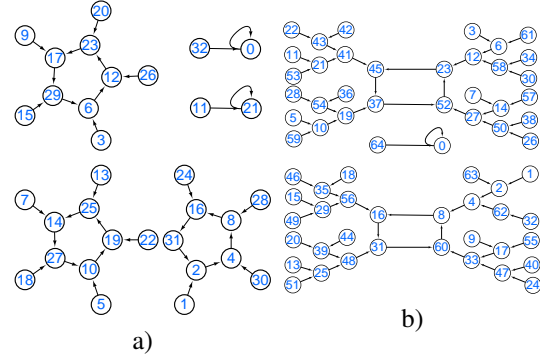


Fig. 6. The SMN of the Tent map with $\mu = 31/2^5$: a) 5-bit precision; b) 6-bit precision.

where $i \in \{0, \dots, 2^n - 1\}$.

Proof. The proof is very similar to that of Corollary 1. Since $(N_\mu / 2^{n\mu-1}) \in [0, 2]$, one has

$$\begin{aligned} & |F_{n+1}^*(2i+1) - 2 \cdot F_n^*(i)| \\ & \leq |R(N_\mu / 2^{n\mu-1})| + \\ & \quad \begin{cases} 2 & \text{if } r_n \in [0.25, 0.75); \\ 1 & \text{otherwise,} \end{cases} \\ & \leq \begin{cases} 4 & \text{if } r_n \in [0.25, 0.75); \\ 3 & \text{otherwise.} \end{cases} \end{aligned}$$

\square

From the proof of Corollary 3, one can see that the upper bound of $|F_{n+1}^*(2i+1) - 2 \cdot F_n^*(i)|$ depends only on N_μ . Figure 7a) depicts the values of $|F_{n+1}^*(2i+1) - 2 \cdot F_n^*(i)|$ and $F_{n+1}^*(2i) - 2F_n^*(i)$ for every node shown in Fig. 6, which agrees with Property 1 and Corollary 1. The corresponding data with $n = 6$ are shown in Fig. 7b), to further demonstrate the differences between F_n^* and F_{n+1}^* .

Now, one can see that the Tent map also follows Property 4, just as the Logistic map, in the same digital domain.

Property 5. *The degree of the SMN of the Tent map has only three possible values:*

$$k = \begin{cases} 1 & \text{the node denoting maximal value;} \\ 2 & \text{other nodes owing pre-images;} \\ 0 & \text{other nodes.} \end{cases}$$

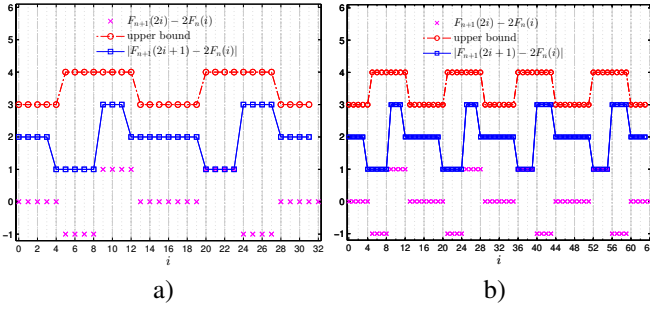


Fig. 7. Distributions of the differences between F_n^* and F_{n+1}^* : a) $n = 5$; b) $n = 6$.

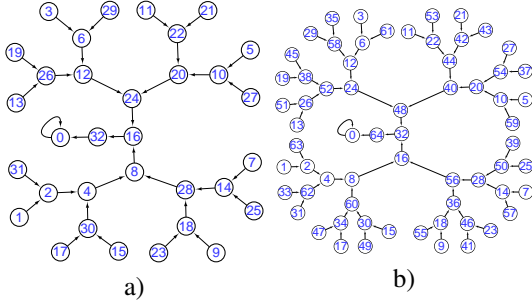


Fig. 8. SMN of the Tent map of $\mu = 1$ with round quantization: a) 5-bit precision; b) 6-bit precision.

Proof. When $x = 1/2$, the maximum value $f(x) = \mu$ is obtained. The node corresponding to $x = 1/2$ only points to one node corresponding to $y = \mu$. So, the in-degree of the node to which $y = \mu$ belongs is $k = 1$.

Due to the symmetry property of the Tent map, only the left half part of the definition domain is considered. In the interval $[0, 1/2]$, the inverse function of the Tent map $y = f(x)$ is

$$f^{-1}(y) = y / (2\mu).$$

As $f'(x) = 2\mu > 0$ for $x \in [0, 1/2]$, $f(x)$ monotonously increases with respect to x . Similar to the proof of Theorem 1, one has the in-degree of the node to which y belongs, as

$$\begin{aligned} k &= 2 \cdot \left\lceil \frac{f^{-1}(y) - f^{-1}(y - (1/2^n))}{2^{-n}} \right\rceil \\ &= 2 \cdot \left\lceil \frac{y/(2\mu) - (y - 1/2^n)/(2\mu)}{2^{-n}} \right\rceil \\ &= 2 \cdot \lceil 1/(2\mu) \rceil \\ &= 2 \end{aligned}$$

when $y \neq \mu$. \square

From Property 5, the edges among the nodes of the SMN of the Tent map are not accumulated as the implementation precision increases (see Fig. 9), which is different from that of the Logistic map.

Based on the above discussions, one can conclude that $f''(x) > 0$ in the whole definition domain is only a sufficient but not a necessary condition for that the associate SMN of the corresponding map follows a power-law distribution.

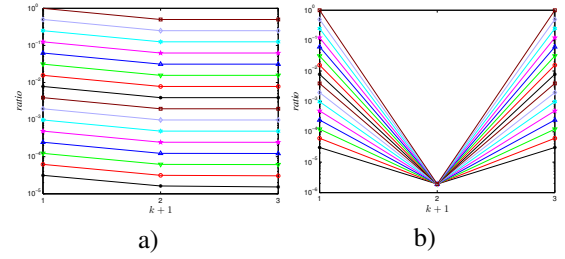


Fig. 9. Statistics of SMN $F_5^* \sim F_{20}^*$ with $\mu = 31/2^5$: a) accumulative in-degree distribution; b) in-degree distribution.

III. ANALYSIS OF THE SMN OF DIGITAL CHAOTIC MAPS IN FLOATING-POINT ARITHMETIC DOMAIN

A. Influence caused by floating-point arithmetic

To obtain a trade-off between the range and the precision, digital computers adopt two kinds of binary representation formats to represent real numbers: fixed-point format and floating-point format. The former is more suitable for integers or real numbers with a fixed precision, and the latter approximate real numbers with a higher and variable precision. Before standardization by IEEE and ANSI in 1985, different machines may use dramatically different representation forms for the floating-point arithmetic.

Following the floating-point standards, a sequence of n bits, $\{b(i)\}_{i=0}^{n-1}$, is divided into three parts: a sign, a signed exponent, and a significand. The represented number is interpreted as the signed product of the significand and the number 2 to the power of its exponent:

$$v = \begin{cases} 0 & \text{if } e = 0, os = 0; \\ (-1)^s \cdot \left(\sum_{i=1}^m b_{l+i} \cdot 2^{-i} \right) \cdot 2^{2-2^{l-1}} & \text{if } e = 0, os \neq 0; \\ (-1)^s \cdot \infty & \text{if } e = 2^l - 1, os = 0; \\ \text{"not a number"} & \text{if } e = 2^l - 1, os \neq 0; \\ (-1)^s \cdot \left(1 + \sum_{i=1}^m b_{l+i} \cdot 2^{-i} \right) \cdot 2^{e-os} & \text{otherwise,} \end{cases}$$

where $s = b_0$, $e = \sum_{i=0}^{l-1} b_{1+i} \cdot 2^i$, $os = 2^{l-1} - 1$.

As to the single-precision floating-point format (binary32), e.g. “float” in C-language and “single” in Matlab, $(l, m) = (8, 23)$, whereas $(l, m) = (11, 52)$ in double-precision floating-point format (binary64). In IEEE 754-2008, half-precision floating-point format (binary16) is designed for storage with a higher precision, not for performing arithmetic computations, where $(l, m) = (5, 10)$. Meanwhile, due to the intermediate scale of the data generated by binary16, its simulation is widely adopted for experiments [50].

In the floating-point arithmetic domain, equality (9) does not exist in general. Some concrete intermediate data during calculating the Logistic map are shown in Table I. Specifically,

$$\mu \cdot x \cdot (1-x) \stackrel{?}{=} \mu \cdot (1-x) \cdot (1 - (1-x)),$$

which is caused by the difference between $fl(x)$ and $fl(1 - fl(1 - fl(x)))$, where $fl(x)$ denotes the normalized floating point number closest to x in the given floating-point domain.

If a number falls into the interval $[0.5, 1]$, its complement in terms of subtraction from 1 in that domain is fixed, so

$$f(1 - f(1 - f(x))) \equiv \begin{cases} 1 - f(1 - f(x)) & \text{if } x \leq 0.5; \\ f(x) & \text{if } x > 0.5. \end{cases} \quad (12)$$

For any $x \in \mathbb{R} \cap [0, 1]$, there exists a unique integer e such that $x = (\sum_{i=0}^{\infty} x_i \cdot 2^{-i}) \cdot 2^e$, where $x_0 = 1$. In the floating-point domain with parameter (l, m) , it becomes

$$f(x) = \begin{cases} (\sum_{i=1}^m x_i \cdot 2^{-i}) \cdot 2^{2-2^{l-1}} & \text{if } x \in (0, 2^{2-2^{l-1}}); \\ (1 + \sum_{i=1}^m x_i \cdot 2^{-i}) \cdot 2^e & \text{if } x \in [2^e, 2^{e+1}), \end{cases}$$

where $e \in \{2 - 2^{l-1}, \dots, -2\}$. Then, one has

$$1 - f(x) = \begin{cases} \sum_{i=1}^{2^{l-1}-2} 2^{-i} + (\sum_{i=1}^m \bar{x}_i \cdot 2^{-i} + 2^{-m}) \cdot 2^{2-2^{l-1}} & \text{if } x \in (0, 2^{2-2^{l-1}}); \\ \sum_{i=1}^{-(e+1)} 2^{-i} + (\sum_{i=1}^m \bar{x}_i \cdot 2^{-i} + 2^{-m}) \cdot 2^e & \text{if } x \in [2^e, 2^{e+1}), \end{cases} \quad (13)$$

where $\bar{x}_i = 1 - x_i$. Observing the first item of the right-hand side of Eq. (13), one can see that the exponent for the representation of $(1 - f(x))$ in that domain is minus one, namely,

$$f(1 - f(x)) = \left(1 + \sum_{i=1}^m \hat{x}_i \cdot 2^{-i}\right) \cdot 2^{-1},$$

where $\hat{x}_i \in \{0, 1\}$. In addition, $2^{l-1} - 2 \geq m + 1$ is a necessary condition for ensuring a sufficient scope of represented numbers by the floating-point format. So, the two cases in Eq. (13) need to be further divided into three cases:

$$f(1 - f(x)) = \begin{cases} (\sum_{i=1}^{m+1} 2^{-i}) & \text{if } x \in (0, 2^{2-2^{l-1}}); \\ (\sum_{i=1}^{m+1} 2^{-i}) & \text{if } x \in [2^{e_1}, 2^{e_1+1}); \\ (\sum_{i=1}^{-e_2-1} 2^{-i}) + (\sum_{i=1}^{m+1+e_2} \bar{x}_i \cdot 2^{-i}) \cdot 2^{e_2} & \text{if } x \in [2^{e_2}, 2^{e_2+1}), \end{cases} \quad (14)$$

where $e_1 \in \{2 - 2^{l-1}, \dots, -m - 2\}$, $e_2 \in \{-m - 1, \dots, -2\}$.

Referring to the first case in Eq. (12) and subtracting Eq. (14) from Eq. (13), one obtains

$$\begin{aligned} & f(1 - f(1 - f(x))) - f(x) \\ &= (1 - f(x)) - f(1 - f(x)) \\ &= \begin{cases} (\sum_{i=m+2}^{2^{l-1}-2} 2^{-i}) + (\sum_{i=1}^m \bar{x}_i \cdot 2^{-i} + 2^{-m}) \cdot 2^{2-2^{l-1}} & \text{if } x \in (0, 2^{2-2^{l-1}}); \\ (\sum_{i=m+2}^{-(e_1+1)} 2^{-i}) + (\sum_{i=1}^m \bar{x}_i \cdot 2^{-i} + 2^{-m}) \cdot 2^{e_1} & \text{if } x \in [2^{e_1}, 2^{e_1+1}); \\ (\sum_{i=m+2+e_2}^m \bar{x}_i \cdot 2^{-i} + 2^{-m}) \cdot 2^{e_2} & \text{if } x \in [2^{e_2}, 2^{e_2+1}). \end{cases} \end{aligned} \quad (15)$$

From Eq. (15), it follows that the difference between $1 - (1 - x)$ and x decreases monotonically in every selected interval, which is verified by the differences shown in Fig. 10. As shown in the inset in Fig. 10, the two segments corresponding the first two cases in

Eq. (15), *i.e.* intervals $[2^{-10+2-2^4}, 2^{2-2^4}] = [2^{-24}, 2^{-14}]$ and $\{[2^{e_1}, 2^{e_1+1}]\}_{e_1=2-2^4}^{-10-2} = \{[2^{e_1}, 2^{e_1+1}]\}_{e_1=-14}^{-12}$ can be connected smoothly. The corresponding difference yielding the final result of the Logistic map is shown in Fig. 11.

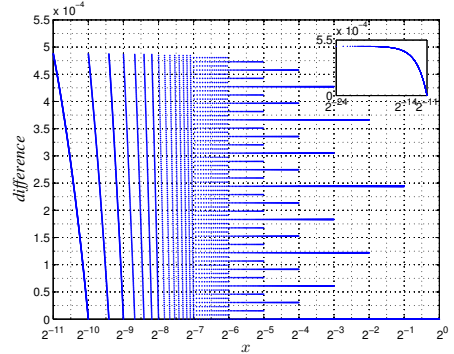


Fig. 10. Subtracting x from $1 - (1 - x)$ under various values of x in Binary16.

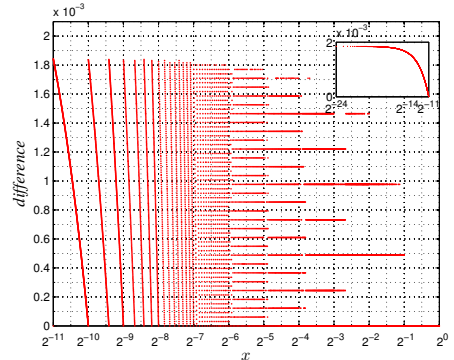


Fig. 11. Subtracting $f(x)$ from $f(1 - x)$ under various values of x in Binary16.

Assume the initial condition $x(0) = (0.b_1 b_2 \dots b_j \dots b_{L-1} b_L)_2 \neq 0$, where $b_L = 1$ (the least significant 1-bit) and $1 - x(0) = (0.b'_1 b'_2 b'_3 \dots b'_j \dots b'_{L-1} b'_L)_2$. Then, the iteration of the Tent map becomes

$$x(1) = \begin{cases} 2x(0) = x(0) \ll 1 = (0.b_2 \dots b_j \dots b_{L-1} b_L)_2, & \text{if } 0 \leq x(0) < 0.5, \\ 2(1 - x(0)) = (b'_1 b'_2 b'_3 \dots b'_j \dots b'_{L-1} b'_L)_2, & \text{if } 0.5 \leq x(0) \leq 1, \end{cases}$$

where \ll denotes the left bit-shifting operation. Note that $b_1 = 0$ when $0 \leq x(0) < 0.5$. Apparently, after $L - 1$ iterations, one obtains $x(L - 1) \equiv (0.b_L)_2 = (0.1)_2$. Then, $x(L) \equiv 1$ and $x(L + 1) \equiv 0$. That is, the number of required iterations converging to zero is $N_r = L + 1$. Note that $N_r = 0$ when $x(0) = 0$. To visualize the operations of the digital Tent map with a typical example, here the evolution process of the number is presented corresponding to the node labeled with "13" in Fig. 12a): $(0.01101)_2 \rightarrow (0.1101)_2 \rightarrow (0.011)_2 \rightarrow (0.11)_2 \rightarrow (0.1)_2 \rightarrow (1)_2 \rightarrow (0)_2$.

From the above analysis, it is clear that no any quantization error is introduced into the digital chaotic iterations, because the chaotic iterations can be exactly carried out with the digital operation \ll . The value of L can be estimated according to two different conditions of $x(0) \neq 0$:

TABLE I
INTERMEDIATE VALUES OF CALCULATING THE LOGISTIC MAP IN BINARY16.

x	$1-x$	$1-(1-x)$	$f(x)$	$f(1-x)$
0.0099945068359375	0.98974609375	0.01025390625	0.037384033203125	0.038360595703125
0.04998779296875	0.94970703125	0.05029296875	0.179443359375	0.1805419921875
0.0899658203125	0.90966796875	0.09033203125	0.309326171875	0.310546875
0.0999755859375	0.89990234375	0.10009765625	0.340087890625	0.340576171875
0.199951171875	0.7998046875	0.2001953125	0.6044921875	0.60498046875
0.289794921875	0.7099609375	0.2900390625	0.77783203125	0.7783203125
0.389892578125	0.60986328125	0.39013671875	0.89892578125	0.8994140625
0.489990234375	0.509765625	0.490234375	0.9443359375	0.94482421875

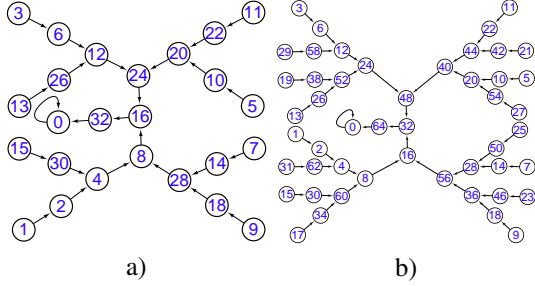


Fig. 12. SMN of the Tent map of $\mu = 1$ in the binary floating-point domain: a) 7-bit binary floating-point domain with $(l = 3, m = 3)$; b) 8-bit binary floating-point domain with $(l = 3, m = 4)$.

- $x(0)$ is a normalized number: $x(0) = (1.b_{m-1} \cdots b_0) \times 2^{-e} = (0.0 \cdots 0 \overset{e-1}{1} b_{m-1} \cdots b_0)_2$. Assuming that the least 1-bit of $x(0)$ is $b_i = 1$, one can immediately get $x(0) = (0.0 \cdots 0 \overset{e-1}{1} \underbrace{b_{m-1} \cdots b_i}_{m-i} \overset{i}{0} \cdots 0)_2$ and deduce $L = (e-1) + 1 + (m-i) = e + (m-i)$. Considering $e \in [1, 2^{l-1} - 2]$ and $i \in [0, m-1]$, one has $L \in [2, 2^{l-1} - 2 + m]$.
- $x(0)$ is a non-zero denormalized number: $x(0) = \frac{(0.b_{m-1} \cdots b_0) \times 2^{2-2^{l-1}}}{2^{l-1-2}} = (0.0 \cdots 0 \overset{2^{l-1-2}}{b_{m-1} \cdots b_i}_{m-i} \overset{i}{0} \cdots 0)_2$. Assuming that the least 1-bit of $x(0)$ is $b_i = 1$, one can immediately get $x(0) = (0.0 \cdots 0 \overset{2^{l-1-2}}{b_{m-1} \cdots b_i}_{m-i} \overset{i}{0} \cdots 0)_2$ and deduce $L = 2^{l-1-2} + (m-i) = 2^{l-1-2} + m - i$. Considering $i \in [0, m-1]$, one has $L \in [2^{l-1} - 1, 2^{l-1} - 2 + m]$.

Summarizing, in both conditions, $L \leq 2^{l-1} - 2 + m$.

Next, we consider the mathematical expectation of $i \in \{0, \dots, m-1\}$. Without loss of generality, for a denormalized number or a normalized number with a fixed exponent e , assume that the mantissa fraction $(b_{m-1} \cdots b_0)_2$ distributes uniformly over the discrete set $\{0, \dots, 2^m - 1\}$. Then, the probability that $(b_i = 1, b_{i-1} = \dots = b_0 = 0)$ is $\frac{1}{2^{i+1}}$, and the probability that $(b_{m-1} = \dots = b_0 = 0)$ is $\frac{1}{2^m}$. Thus, the mathematical expectation of i is

$$\begin{aligned}
 E(i) &\approx \sum_{i=0}^{m-1} i \cdot \frac{1}{2^{i+1}} + m \cdot \frac{1}{2^m} \\
 &= \frac{1}{2} \cdot \sum_{i=1}^{m-1} \frac{i}{2^i} + \frac{m}{2^m} \\
 &= 1 - \frac{1}{2^m} \dots
 \end{aligned}$$

Then, we analyse the mathematical expectation of $e \in \{1, \dots, 2^{l-1} - 2\}$. From the uniform distribution of $x(0)$ in the interval $[0, 1]$, it follows that the probability of the exponent e is about $\text{Prob}[2^{-e} \leq x < 2^{-(e-1)}] = 2^{-e}$. Thus, the mathematical expectation of e is

$$E(e) \approx \sum_{e=1}^{2^{l-1}-2} \frac{e}{2^e} = 2 - \frac{2^{l-1}}{2^{2^{l-1}-2}} \approx 2.$$

From the above deductions, one can immediately deduce that

$$\begin{aligned}
 E(L) &= \text{Prob}[\text{normalized numbers}] \cdot (E(e) + (m - E(i))) + \\
 &\quad \text{Prob}[\text{denormalized numbers}] \cdot (2^{l-1} - 2 + m - E(i)) \\
 &= \frac{2^{l-1} - 2}{2^{l-1} - 1} \cdot (E(e) + (m - E(i))) + \\
 &\quad \frac{1}{2^{l-1} - 1} \cdot (2^{l-1} - 2 + m - E(i)) \\
 &\approx \frac{2^{l-1} - 2}{2^{l-1} - 1} \cdot (2 + (m - 1)) + \frac{1}{2^{l-1} - 1} \cdot (2^{l-1} - 2 + m - 1) \\
 &= \frac{(2^{l-1} - 2)(m + 2) + m - 1}{2^{l-1} - 1}. \tag{16}
 \end{aligned}$$

To verify the mathematical expectation of N_r , some experiments were performed for testing on 10,000 initial conditions, pseudo-randomly generated with the standard Rand function of Microsoft Visual Studio 2010. The occurrence frequency of different values is shown in Fig. 13, where the average values of N_r for the three arithmetical domains are about 11.95, 24.97, and 54.01, respectively. Every distribution well agrees with the theoretical expectations.

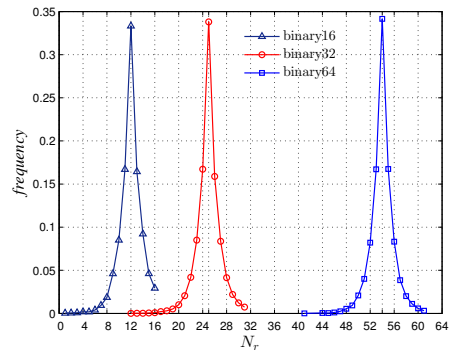


Fig. 13. The occurrence frequency of different values of N_r within a total of 10,000 values.

B. Relationship between the SMN obtained in two arithmetic domains

In the floating-point arithmetic domain with the exponent width of l bits and the mantissa width of m bits, the minimum fixed interval is $2^{(1-(2^{l-1}-1))} \cdot 2^{-m} = 2^{2-2^{l-1}-m}$. Under a fixed-point computing environment of precision n , fixed interval is 2^{-n} . If $2^{2-2^{l-1}-m} = 2^{-n}$, namely, $n = m + 2^{l-1} - 2$, the two SMN obtained by implementing one map in the two domains have a strong correlation, as shown in the following theorem.

Theorem 2. Given binary floating-point format parameters l and m , the node with the label i in $F_{l,m}$ and that with the label i in F_n satisfy

$$F_n(i) - F_{l,m}(i) \leq \begin{cases} 1 & \text{if } F_n(i) \in [0, 2^m); \\ 2^{n-m-1-j} & \text{if } F_n(i) \in [2^{n-j-1}, 2^{n-j}), \end{cases} \quad (17)$$

where $j \in \{2^{l-1} - 3, 2^{l-1} - 4, \dots, 1, 0\}$, and

$$n = m + 2^{l-1} - 2. \quad (18)$$

Proof. Utilizing the property of the integer quantization function

$$|x - R(y)| = |R(x - y)|, \quad x \in \mathbb{Z},$$

one gets

$$\begin{aligned} |F_{l,m}(i) - F_n(i)| &= |f_{l,m}(i) \cdot 2^n - R(f_n(i) \cdot 2^n)| \\ &= |R((f_{l,m}(i) - f_n(i)) \cdot 2^n)|, \end{aligned}$$

where $F_{l,m}(i) = f_{l,m}(i) \cdot 2^n$.

As for the node labeled with “ i ” in F_n , the corresponding value $i/2^n$ can be accurately represented in both the floating-point domain with (l, m) and the n -bit fixed-point domain. Furthermore, the intermediate processes of calculating $f(i/2^n)$ are the same in the two arithmetic domains. So, the difference between $f_{l,m}(i)$ and $f_n(i)$ is only caused by the final quantization step.

When $F_n(i) \in [2^{n-1-j}, 2^{n-j})$, one has

$$\begin{aligned} f_{l,m}(i) &= 2^{-j-1} \cdot \left(1 + \sum_{i=1}^m a_i \cdot 2^{-i} \right), \\ f_n(i) &= 2^{-j-1} \cdot \left(1 + \sum_{i=1}^n c_i \cdot 2^{-i} \right), \end{aligned}$$

where $j \in \{0, \dots, 2^{l-1} - 3\}$. Obviously, $a_i = c_i$ for $i = 1 \sim m$. So, one has

$$\begin{aligned} f_n(i) - f_{l,m}(i) &= 2^{-j-1} \cdot \left(\sum_{i=m+1}^n c_i \cdot 2^{-i} \right) \\ &< 2^{-m-j-1}. \end{aligned}$$

Then, one can conclude that

$$\begin{aligned} F_n(i) - F_{l,m}(i) &= R((f_n(i) - f_{l,m}(i)) \cdot 2^{m+1+j} \cdot 2^{n-m-1-j}) \\ &\leq R(2^{n-m-1-j}) \\ &= 2^{n-m-1-j}. \end{aligned}$$

When $F_n(i) \in [0, 2^m)$, $f_{l,m}(i)$ is a subnormal number, and $f_{l,m}(i)$ and $f_n(i)$ can be expressed as

$$\begin{aligned} f_{l,m}(i) &= 2^{2-2^{l-1}} \cdot \left(\sum_{i=1}^m a_i \cdot 2^{-i} \right), \\ f_n(i) &= 2^{2-2^{l-1}} \cdot \left(\sum_{i=1}^n c_i \cdot 2^{-i} \right). \end{aligned}$$

Similarly to the above cases, one has

$$\begin{aligned} f_n(i) - f_{l,m}(i) &= 2^{2-2^{l-1}} \cdot \left(\sum_{i=m+1}^n c_i \cdot 2^{-i} \right) \\ &< 2^{-m+2-2^{l-1}} \\ &= 2^{-n}. \end{aligned}$$

So, one gets

$$\begin{aligned} |F_{l,m}(i) - F_n(i)| &= R(|(f_{l,m}(i) - f_n(i)) \cdot 2^n|) \\ &\leq R(1) = 1. \end{aligned}$$

□

To illustrate Theorem 2, we draw three connected components of SMN of the Logistic map with $\mu = 121/2^5$, F_{12} , in Fig. 14a). Relative relations of the nodes in $F_{4,6}$ are shown in Fig. 14b). The corresponding parts of $F_{4,6}$ are shown in Fig. 14b).

Due to the space limitation, only the involved nodes and their neighbors, but not the original connected components, are shown in Fig. 14b). Moreover, differences between some mapping in F_{12} and that in $F_{4,6}$ are listed in Table II, which validates Theorem 2 as well.

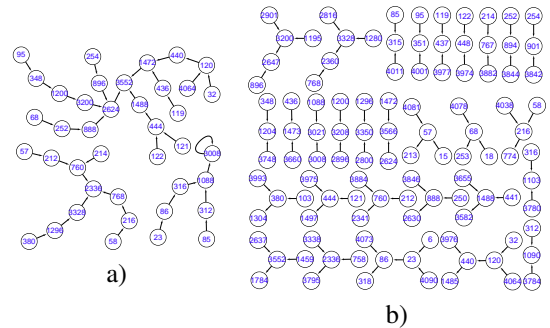


Fig. 14. Some connected components of SMN of the Logistic map in floating-point domain and relative relations of their nodes in the corresponding fixed-point domain: a) 11-bit floating-point domain with $(l = 4, m = 6)$; b) 12-bit finite-precision domain, where $\mu = 121/2^5$.

From Theorem 2, one can see that SMN of the Logistic map implemented by the floating-point arithmetic (m, l) can be regarded as a rewired version of the sub-network of its SMN implemented in the corresponding fixed-point precision.

TABLE II
DIFFERENCES BETWEEN SMN IMPLEMENTED IN TWO ARITHMETIC
DOMAINS WITH $n = 12, l = 4, m = 6$.

i	$F_n(i)$	$F_{l,m}(i)$	$F_n(i) - F_{l,m}(i)$	$2^{n-m-1-j}$
6	23	22	1	1
18	68	67	1	1
33	124	123	1	1
40	150	148	2	2
53	198	196	2	2
67	249	248	2	2
82	304	300	4	4
112	412	408	4	4
130	476	472	4	4
156	567	560	7	8
238	848	840	8	8
284	999	992	7	8
316	1103	1088	15	16
576	1872	1856	16	16
648	2063	2048	15	16
768	2360	2336	24	32
1280	3328	3296	32	32
2080	3871	3840	31	32

More precisely, SMN $F_{l,m}$ can be generated from SMN F_n as follows: all nodes linking to $F_n(i)$ are redirected to the node labeled $2^{n-j} - (k+1) \cdot 2^{n-m-1-j}$ when $2^{n-j} - (k+1) \cdot 2^{n-m-1-j} < F_n(i) < 2^{n-j} - k \cdot 2^{n-m-1-j}$; all nodes linking to $F_n(i)$, except the node labeled 2^n , are redirected to the nodes with label $2^{n-j} - k \cdot 2^{n-m-1-j}$ or $2^{n-j} - (k+1) \cdot 2^{n-m-1-j}$ when $F_n(i) = 2^{n-j} - k \cdot 2^{n-m-1-j}$, where $j \in \{2^{l-1} - 4, \dots, 1, 0\}$, and $k = 0 \sim 2^m - 1$. When $0 < F_n(i) < 2^{m+1}$, all nodes linking to $F_n(i)$ are redirected to the nodes with label $F_n(i)$ or $F_n(i) - 1$.

The process can be verified by comparing Fig. 15a) and Fig. 15b) with Fig. 16a) and Fig. 16b), respectively. Table III presents the differences between the two SMN in the two arithmetic domains with $n = 6$, and $(l, m) = (3, 4)$.

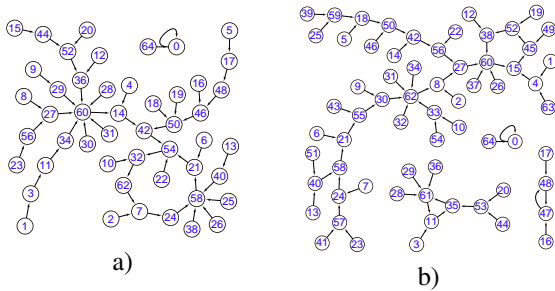


Fig. 15. SMN of the Logistic map with $\mu = 62/2^4$: a) 8-bit floating-point domain with $(l = 3, m = 4)$; b) 6-bit fixed-point precision and round quantization.

Referring to Theorems 1 and 2, one can conclude that the cumulative in-degree distribution and the in-degree distribution of the SMN of the Logistic map implemented in the floating-point arithmetic domain approximate that implemented in the corresponding fixed-point arithmetic domain. This is verified by comparing Fig. 4 and Fig. 17 with Fig. 5 and Fig. 18, respectively.

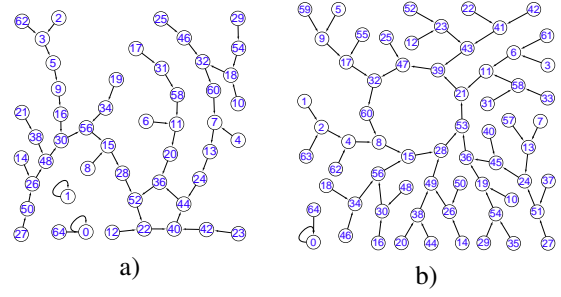


Fig. 16. SMN of the Tent map with $\mu = 15/2^4$: a) 8-bit binary floating-point domain with $(l = 3, m = 4)$; b) 6-bit fixed-point precision and round quantization.

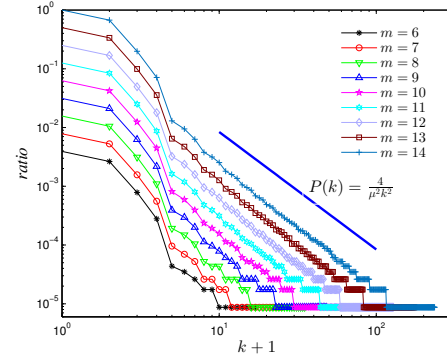


Fig. 17. Cumulative in-degree distributions of the SMN of the Logistic map in various floating-point domains, where $l = 4, m = 6 \sim 14$.

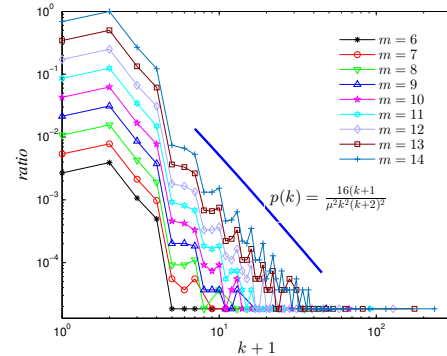


Fig. 18. In-degree distributions of the SMN of the Logistic map in various floating-point domains, where $l = 4, m = 6 \sim 14$.

IV. TESTING THE RANDOMNESS OF VARIOUS PRNG BASED ON CHAOS VIA SMN

This section demonstrates that SMN can be used to classify the structure of various PRNG based on iterating a chaotic map. Furthermore, it can work as a coarse visual tool on evaluating their randomness levels, as a complementary to all kinds of test indexes enclosed in the standard test suites, *e.g.* NIST SP 800-22 [51] and TestU01 [52]. For this purpose, the various methods chaos-based PRNG are classified as the following six categories by scrutinizing the SMN of enhanced Logistic maps:

- *Selecting state and control parameters*

By observing Fig. 1, one can see that the nodes labeled “0” and “ 2^n ” are pathological seeds, therefore they should be excluded from any PRNG. More similar nodes can be

TABLE III
DIFFERENCES BETWEEN SMN IMPLEMENTED IN THE TWO ARITHMETIC DOMAINS WITH $n = 6, l = 3, m = 4$.

i	$F_n(i)$	$f_n(i) - f_{l,m}(i)$	$2^{-(m+1+j)}$	i	$F_n(i)$	$f_n(i) - f_{l,m}(i)$	$2^{-(m+1+j)}$	i	$F_n(i)$	$f_n(i) - f_{l,m}(i)$	$2^{-(m+1+j)}$
0	0	0	0.015625	16	30	0	0.015625	32	60	0	0.03125
1	2	0.013671875	0.015625	17	32	0.013671875	0.03125	34	56	0.00390625	0.03125
2	4	0.01171875	0.015625	18	34	0.02734375	0.03125	36	53	0.0078125	0.03125
3	6	0.009765625	0.015625	19	36	0.025390625	0.03125	38	49	0.01171875	0.03125
4	8	0.0078125	0.015625	20	38	0.0234375	0.03125	40	45	0.015625	0.03125
5	9	0.005859375	0.015625	21	39	0.021484375	0.03125	42	41	0.01953125	0.03125
6	11	0.00390625	0.015625	22	41	0.01953125	0.03125	44	38	0.0234375	0.03125
7	13	0.001953125	0.015625	23	43	0.017578125	0.03125	46	34	0.02734375	0.03125
8	15	0	0.015625	24	45	0.015625	0.03125	48	30	0	0.015625
9	17	0.013671875	0.015625	25	47	0.013671875	0.03125	50	26	0.00390625	0.015625
10	19	0.01171875	0.015625	26	49	0.01171875	0.03125	52	23	0.0078125	0.015625
11	21	0.009765625	0.015625	27	51	0.009765625	0.03125	54	19	0.01171875	0.015625
12	23	0.0078125	0.015625	28	53	0.0078125	0.03125	56	15	0	0.015625
13	24	0.005859375	0.015625	29	54	0.005859375	0.03125	58	11	0.00390625	0.015625
14	26	0.00390625	0.015625	30	56	0.00390625	0.03125	60	8	0.0078125	0.015625
15	28	0.001953125	0.015625	31	58	0.001953125	0.03125	62	4	0.01171875	0.015625

found in Fig. 1c), which are very difficult to be found via a randomness test suite. In [12], it was claimed that the discrete Tent map can achieve a satisfactory trade-off among the period lengths, the statistical characteristics of the generated bit sequences, and the complexity of hardware implementations in the fixed-point domain. As the control parameter is the sole factor in the SMN of the Tent map under the given implementation environment, in [16] it only selects the desired SMN by choosing some control parameters.

- *Increasing the arithmetic precision*

As discussed in [9], increasing the arithmetic precision can substantially enlarge the average length of the orbit of SMN and enhance its complexity. However, from Property 4, one can see that it cannot change its overall structure, as can be observed from Fig. 1. Figure 2 in [6] also confirms that increasing the precision does not always enlarge the average path period of SMN. In addition, exhaustively searching smaller-scale data incurred by a lower arithmetic precision, *e.g.* binary16, may also find the rules found from the big data generated by a higher-precision as in [6].

- *Perturbing states*

Essentially, perturbing the state is to jump from a walk path in SMN to another (namely, to rewire the linking edges of SMN) [16]–[18], [43]. To show the effect of this kind of methods, SMN is perturbed as shown in Fig. 1b), by the method given in [43]. The result is presented in Fig. 19a), where the perturbation is performed by bit-wise XOR of the three least significant bits of the mapping value and the perturbing bit sequence $(100)_2$. From Fig. 19a), one can see that the orbit starting from some states, especially that in connected components of small sizes, remains unchanged. A cycle may become even shorter after the states are perturbed. Generally, the enhancing methods based on feedback control proposed in [13], [48] can be considered as perturbing nodes of SMN adaptively.

- *Perturbing the control parameters*

Perturbing the control parameters is to walk from a path of SMN corresponding to one control parameter to that corresponding to another one by a timely jump. So, this kind

of methods is actually to cascade multiple SMN generated by the same chaotic map [44, Sec. 4]. To visualize this strategy, SMN cascades are shown in Fig. 1b), along with that in Fig. 15b), and the results are presented in Fig. 19b).

- *Switching among multiple chaotic maps*

In each iteration, the chaotic map is switched from one candidate to another, so as to generate the next state [46], [47]. From the viewpoint of SMN, the obtained orbit is to walk on every SMN one step and then jump to another SMN, depending on the switching operation. As one state may be operated by different chaotic maps, the out-degrees of some nodes of the final SMN may be larger than 1 and bounded by the number of available chaotic maps. A demo on switching between the Logistic map and the Tent map is shown in Fig. 19c).

- *Cascading among multiple chaotic maps*

This kind of methods is to cascade some walks on multiple SMN into one walk [45]. The method used in [16] is an extreme case, where the outputs of one chaotic map are used to select the start of the path in SMN of another chaotic map. Although two chaotic maps were used, the finally obtained SMN is not updated. A demo of the SMN, on cascading two chaotic maps shown in Fig. 1b) and Fig. 6 respectively, is depicted in Fig. 19d). The isolated connected components in the original SMN can be connected into the final cascaded SMN once they own one pair of nodes connected in any SMN.

V. CONCLUSIONS

This paper has studied the dynamical properties of digital chaotic maps with the methodology of complex networks. Some subtle properties of the state-mapping networks of the Logistic map and the Tent map have been revealed, offering a panorama with both microscopic and macroscopic structures of the network. It has been demonstrated that the state-mapping network of digital maps in a small-precision digital domain can work as an efficient tool to classify its structure and coarsely verify its randomness. This analysis method can be further extended to higher-dimensional chaotic systems.

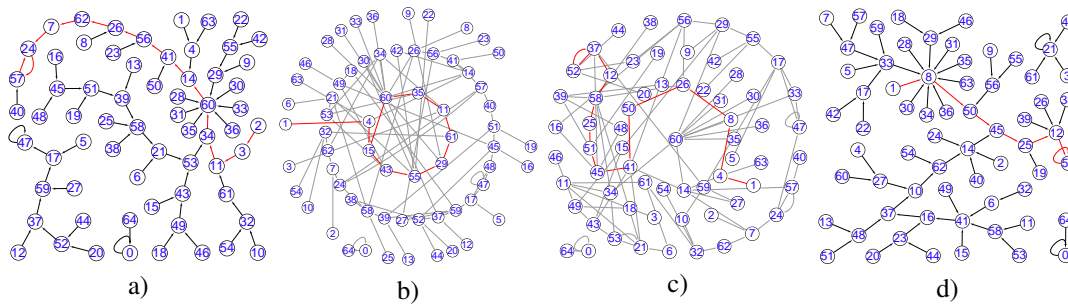


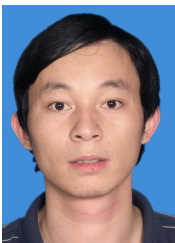
Fig. 19. Results of enhancing SMN shown in Fig. 1b) with various methods: a) perturbing states with the method in [43]; b) perturbing control parameter μ from $121/2^5$ to $62/2^4$; c) switching with SMN of the Tent map with parameter $\mu = 31/2^5$ alternately; d) cascading with SMN of the Tent map with parameter $\mu = 31/2^5$.

Achievements notwithstanding, more properties and applications of the state-mapping network framework of various chaotic maps call for further exploration in the near future.

REFERENCES

- [1] D. F. Voss, "Chaos on computers," *Science*, vol. 246, no. 4934, pp. 1172–1172, 1989.
- [2] K. Umeno and A.-H. Sato, "Chaotic method for generating q -gaussian random variables," *IEEE Transactions on Information Theory*, vol. 59, no. 5, pp. 3199–3209, 2013.
- [3] J. Oteo and J. Ros, "Double precision errors in the Logistic map: Statistical study and dynamical interpretation," *Physical Review E*, vol. 76, no. 3, p. 036214, 2007.
- [4] Z. Galias, "The dangers of rounding errors for simulations and analysis of nonlinear circuits and systems—and how to avoid them," *IEEE Circuits and Systems Magazine*, vol. 13, no. 3, pp. 35–52, Aug 2013.
- [5] S. C. Phatak and S. S. Rao, "Logistic map: A possible random-number generator," *Physical Review E*, vol. 51, no. 4, pp. 3670–3678, 1995.
- [6] K. Persohn and R. Povinelli, "Analyzing Logistic map pseudorandom number generators for periodicity induced by finite precision floating-point representation," *Chaos Solitons & Fractals*, vol. 45, no. 3, pp. 238–245, 2012.
- [7] C. Grebogi, E. Ott, and J. A. Yorke, "Roundoff-induced periodicity and the correlation dimension of chaotic attractors," *Physical Review A*, vol. 38, no. 7, p. 3688, 1988.
- [8] S. Li, G. Chen, and X. Mou, "On the dynamical degradation of digital piecewise linear chaotic maps," *International Journal of Bifurcation and Chaos*, vol. 15, no. 10, pp. 3119–3151, 2005.
- [9] T. Lin and L. O. Chua, "On chaos of digital filters in the real world," *IEEE Transactions on Circuits and Systems*, vol. 38, no. 5, pp. 557–558, May 1991.
- [10] L. Kocarev, J. Szczepanski, J. M. Amigó, and I. Tomovski, "Discrete chaos-I: Theory," *IEEE Transactions on Circuits and Systems-I: Regular Papers*, vol. 53, no. 6, pp. 1300–1309, Jun 2006.
- [11] L. Kocarev and G. Jakimoski, "Pseudorandom bits generated by chaotic maps," *IEEE Transactions on Circuits and Systems I: Fundamental Theory and Applications*, vol. 50, no. 1, pp. 123–126, Jan 2003.
- [12] T. Addabbo, M. Alioto, A. Fort, S. Rocchi, and V. Vignoli, "The digital Tent map: performance analysis and optimized design as a low-complexity source of pseudorandom bits," *IEEE Transactions on Instrumentation and Measurement*, vol. 55, no. 5, pp. 1451–1458, Oct 2006.
- [13] Y. Deng, H. Hu, W. Xiong, N. N. Xiong, and L. Liu, "Analysis and design of digital chaotic systems with desirable performance via feedback control," *IEEE Transactions on Systems, Man, and Cybernetics: Systems*, vol. 45, no. 8, pp. 1187–1200, Aug 2015.
- [14] N. Masuda and K. Aihara, "Cryptosystems with discretized chaotic maps," *IEEE Transactions on Circuits and Systems I: Fundamental Theory and Applications*, vol. 49, no. 1, pp. 28–40, Jan 2002.
- [15] S. M. Ulam and J. von Neumann, "On combination of stochastic and deterministic processes," *Bulletin of the American Mathematical Society*, vol. 53, no. 11, p. 1120, 1947.
- [16] G. Heidari-Bateni and C. D. McGillem, "A chaotic direct-sequence spread-spectrum communication system," *IEEE Transactions on Communications*, vol. 42, no. 234, pp. 1524–1527, Feb 1994.
- [17] S.-L. Chen, T. Hwang, and W.-W. Lin, "Randomness enhancement using digitalized modified logistic map," *IEEE Transactions on Circuits and Systems II: Express Briefs*, vol. 57, no. 12, pp. 996–1000, Dec 2010.
- [18] C.-Y. Li, Y.-H. Chen, T.-Y. Chang, L.-Y. Deng, and K. To, "Period extension and randomness enhancement using high-throughput reseeding-mixing PRNG," *IEEE Transactions on Very Large Scale Integration (VLSI) Systems*, vol. 20, no. 2, pp. 385–389, Feb 2012.
- [19] M. Jessa, "The period of sequences generated by Tent-like maps," *IEEE Transactions on Circuits and Systems I: Fundamental Theory and Applications*, vol. 49, no. 1, pp. 84–89, Jan 2002.
- [20] —, "Designing security for number sequences generated by means of the sawtooth chaotic map," *IEEE Transactions on Circuits and Systems-I: Regular Papers*, vol. 53, no. 5, pp. 1140–1150, May 2006.
- [21] T. Addabbo, M. Alioto, A. Fort, A. Pasini, S. Rocchi, and V. Vignoli, "A class of maximum-period nonlinear congruential generators derived from the Rényi chaotic map," *IEEE Transactions on Circuits and Systems I: Regular Papers*, vol. 54, no. 4, pp. 816–828, Apr 2007.
- [22] F. Chen, K.-W. Wong, X. Liao, and T. Xiang, "Period distribution of the generalized discrete Arnold Cat map for $N = 2^e$," *IEEE Transactions on Information Theory*, vol. 59, no. 5, pp. 3249–3255, May 2013.
- [23] G. Alvarez and S. Li, "Some basic cryptographic requirements for chaos-based cryptosystems," *International Journal of Bifurcation and Chaos*, vol. 16, no. 8, pp. 2129–2151, 2006.
- [24] R. Sedgewick, T. G. Szymanski, and A. C. Yao, "The complexity of finding cycles in periodic functions," *SIAM Journal on Computing*, vol. 11, no. 2, pp. 376–390, 1982.
- [25] P. Flajolet and A. M. Odlyzko, "Random mapping statistics," in *Advances in Cryptology – Crypto'89*, ser. *Lecture Notes in Computer Science*, vol. 434, 1990, pp. 329–354.
- [26] İ. Öztürk and R. Kiliç, "Cycle lengths and correlation properties of finite precision chaotic maps," *International Journal of Bifurcation and Chaos*, vol. 24, no. 09, p. 1450107, 2014.
- [27] F. Chen, K.-W. Wong, X. Liao, and T. Xiang, "Period distribution of generalized discrete arnold cat map for $n = p^e$," *IEEE Transactions on Information Theory*, vol. 58, no. 1, pp. 445–452, 2012.
- [28] B. Yang and X. Liao, "Period analysis of the Logistic map for the finite field," *Science China Information Sciences*, vol. 60, no. 2, p. 022302, 2017.
- [29] T. Miyazaki, S. Araki, Y. Nogami, and S. Uehara, "Rounding logistic maps over integers and the properties of the generated sequences," *IEICE Transactions on Fundamentals of Electronics, Communications and Computer Sciences*, vol. 94, no. 9, pp. 1817–1825, 2011.
- [30] S. Araki, H. Muraoka, T. Miyazaki, S. Uehara, and K. Kakizaki, "A design guide of renewal of a parameter of the Logistic map over integers on pseudorandom number generator," in *International Symposium on Information Theory and Its Applications*. IEEE, 2016, pp. 781–785.
- [31] J. Zhang and M. Small, "Complex network from pseudoperiodic time series: topology versus dynamics," *Physical Review Letters*, vol. 96, no. 23, p. 238701, 2006.
- [32] P. M. Binder and R. V. Jensen, "Simulating chaotic behavior with finite-state machines," *Physical Review A*, vol. 34, no. 5, pp. 4460–4463, 1986.
- [33] P. Binder, "Limit-cycles in a quadratic discrete iteration," *Physica D*, vol. 57, no. 1-2, pp. 31–38, 1992.
- [34] N. Marwan, J. F. Donges, Y. Zou, R. V. Donner, and J. Kurths, "Complex network approach for recurrence analysis of time series," *Physics Letters A*, vol. 373, no. 46, pp. 4246–4254, 2009.
- [35] R. V. Donner, J. Heitzig, J. F. Donges, Y. Zou, N. Marwan, and J. Kurths,

- "The geometry of chaotic dynamics—a complex network perspective," *European Physical Journal B*, vol. 84, no. 4, pp. 653–672, 2011.
- [36] A. Shreim, P. Grassberger, W. Nadler, B. Samuelsson, J. E. S. Socolar, and M. Paczuski, "Network analysis of the state space of discrete dynamical systems," *Physical Review Letters*, vol. 98, no. 19, p. 198701, 2007.
- [37] B. Luque, L. Lacasa, F. J. Ballesteros, and A. Robledo, "Feigenbaum graphs: a complex network perspective of chaos," *PLoS One*, vol. 6, no. 9, p. art. no. e22411, 2011.
- [38] T. Iba, "Scale-free networks hidden in chaotic dynamical systems," arXiv:nlin/1007.4137, 2010.
- [39] E. Borges, D. Cajueiro, and R. Andrade, "Mapping dynamical systems onto complex networks," *The European Physical Journal B*, vol. 58, no. 4, pp. 469–474, 2007.
- [40] F. Kyriakopoulos and S. Thurner, "Directed network representation of discrete dynamical maps," in *International Conference on Computational Science*, ser. Lecture Notes in Computer Science, vol. 4488. Springer, 2007, pp. 625–632.
- [41] T. Iba, "Hidden order in chaos: The network-analysis approach to dynamical systems," in *Proceedings of the Eighth International Conference on Complex Systems*, 2011, pp. 769–783, <http://necsi.edu/events/iccs2011/papers/70.pdf>.
- [42] X. Xu, J. Zhang, and M. Small, "Superfamily phenomena and motifs of networks induced from time series," *Proceedings of the National Academy of Sciences*, vol. 105, no. 50, pp. 19 601–19 605, 2008.
- [43] T. Sang, R. Wang, and Y. Yan, "Perturbance-based algorithm to expand cycle length of chaotic key stream," *Electronics Letters*, vol. 34, no. 9, pp. 873–874, 1998.
- [44] J. Černák, "Digital generators of chaos," *Physics letters A*, vol. 214, no. 3-4, pp. 151–160, 1996.
- [45] Z. Hua and Y. Zhou, "One-dimensional nonlinear model for producing chaos," *IEEE Transactions on Circuits and Systems I: Regular Papers*, <https://doi.org/10.1109/TCSI.2017.2717943>, 2017.
- [46] N. Nagaraj, M. C. Shastry, and P. G. Vaidya, "Increasing average period lengths by switching of robust chaos maps in finite precision," *The European Physical Journal Special Topics*, vol. 165, no. 1, pp. 73–83, 2008.
- [47] Y. Wu, Y. Zhou, and L. Bao, "Discrete wheel-switching chaotic system and applications," *IEEE Transactions on Circuits and Systems I-Regular Papers*, vol. 61, no. 12, pp. 3469–3477, Dec 2014.
- [48] T. Addabbo, M. Alioto, A. Fort, S. Rocchi, and V. Vignoli, "A feedback strategy to improve the entropy of a chaos-based random bit generator," *IEEE Transactions on Circuits and Systems I: Regular Papers*, vol. 53, no. 2, pp. 326–337, 2006.
- [49] S. Wang, W. Liu, H. Lu, J. Kuang, and G. Hu, "Periodicity of chaotic trajectories in realizations of finite computer precisions and its implication in chaos communications," *International journal of modern physics B*, vol. 18, no. 17, pp. 2617–2622, 2004.
- [50] C. Rau, "Half-precision floating point library," <http://half.sourceforge.net/index.html>, 2017.
- [51] A. Rukhin et al., "A statistical test suite for random and pseudorandom number generators for cryptographic applications," NIST Special Publication 800-22rev1a, 2010, available online at http://csrc.nist.gov/groups/ST/toolkit/rng/documentation_software.html.
- [52] P. L. Ecuyer and R. Simard, "TestU01: A C library for empirical testing of random number generators," *ACM Transactions on Mathematical Software*, vol. 33, no. 4, p. art. no. 22, 2007.



Chengqing Li (M'07-SM'13) received his M.Sc. degree in Applied Mathematics from Zhejiang University, China in 2005 and his Ph.D. degree in Electronic Engineering from City University of Hong Kong in 2008. Thereafter, he worked as a Post-doctoral Fellow at The Hong Kong Polytechnic University till September 2010. Then, he worked at the College of Information Engineering, Xiangtan University, China as an Associate Professor and Full Professor recently. From April 2013 to July 2014, he worked at the University of Konstanz, Germany,

under the support of the Alexander von Humboldt Foundation.

Prof. Li focuses on security analysis of multimedia encryption schemes and privacy protection schemes. He has published about fifty papers on the subject in the past 13 years, receiving more than 1800 citations with h-index 23.



Bingbing Feng is pursuing his M.Sc. degree in computer science at the College of Information Engineering, Xiangtan University, where he received his B.Sc. degree in the same subject in 2015. His research interests include complex networks and nonlinear dynamics.



Shujun Li (M'08-SM'12) received the B.E. degree in information science and engineering, and the Ph.D. degree in information and communication engineering from Xi'an Jiaotong University, China, in 1997 and 2003, respectively. From 2003 to 2005, he was a Post-Doctoral Research Assistant with the City University of Hong Kong. From 2005 to 2007, he was a Post-Doctoral Fellow with The Hong Kong Polytechnic University. From 2007 to 2008, he was a Humboldt Research Fellow with the FernUniversität, Hagen, Germany. From 2008 to 2011, he was a Zukunftscolleg Fellow with the Universität Konstanz, Germany. He currently is a Reader with the University of Surrey, U.K., and a Deputy Directory with the Surrey Centre for Cyber Security.

Dr. Li's current research interests include cyber security and privacy, digital and multimedia forensics, human-centered computing, and visual quality assessment.



Jürgen Kurths received the Ph.D. degree from the GDR Academy of Sciences, Berlin, Germany, in 1983. He was a Full Professor at the University of Potsdam from 1994 to 2008. He has been a Professor of nonlinear dynamics at Humboldt University of Berlin, Berlin, and the Chair of the research domain Transdisciplinary Concepts of the Potsdam Institute for Climate Impact Research, Potsdam, Germany, since 2008. He has authored or coauthored more than 500 papers that are cited more than 18,000 times (H-index: 57). He became a member of the Academy of Europe in 2010 and of the Macedonian Academy of Sciences and Arts in 2012. He is the Editor-in-chief of CHAOS.

Prof. Kurths' primary research interests include synchronization, complex networks, and time-series analysis and their applications.



Guanrong Chen (M'89-SM'92-F'97) received the MSc. degree in computer science from Sun Yat-sen University, Guangzhou, China in 1981 and the Ph.D. degree in applied mathematics from Texas A&M University, Texas, TX, USA in 1987. He has been a Chair Professor and the Director of the Centre for Chaos and Complex Networks, City University of Hong Kong, Hong Kong since 2000, prior to that, he was a tenured Full Professor with the University of Houston, Houston, TX, USA.

Prof. Chen was a recipient of the 2011 Euler Gold Medal, Russia, and Highly Cited Researcher Awards in Engineering as well as in Mathematics by Thomson Reuters, and conferred Honorary Doctorate by the Saint Petersburg State University, Russia in 2011 and by the University of Le Havre, Normandie, France in 2014. He is a member of the Academia of Europe and a fellow of The World Academy of Sciences.